

Defining the Face Processing Network: Optimization of the Functional Localizer in fMRI

Christopher J. Fox,^{1,2*†} Giuseppe Iaria,^{2†} and Jason J.S. Barton²

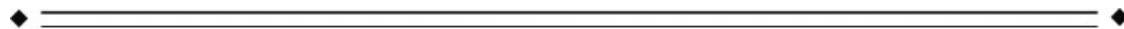
¹Graduate Program in Neuroscience, University of British Columbia, British Columbia, Canada

²Human Vision and Eye Movement Laboratory, Division of Neurology, Department of Ophthalmology and Visual Sciences, Faculty of Medicine, University of British Columbia, British Columbia, Canada



Abstract: Functional localizers that contrast brain signal when viewing faces versus objects are commonly used in functional magnetic resonance imaging studies of face processing. However, current protocols do not reliably show all regions of the core system for face processing in all subjects when conservative statistical thresholds are used, which is problematic in the study of single subjects. Furthermore, arbitrary variations in the applied thresholds are associated with inconsistent estimates of the size of face-selective regions-of-interest (ROIs). We hypothesized that the use of more natural dynamic facial images in localizers might increase the likelihood of identifying face-selective ROIs in individual subjects, and we also investigated the use of a method to derive the statistically optimal ROI cluster size independent of thresholds. We found that dynamic facial stimuli were more effective than static stimuli, identifying 98% (versus 72% for static) of ROIs in the core face processing system and 69% (versus 39% for static) of ROIs in the extended face processing system. We then determined for each core face processing ROI, the cluster size associated with maximum statistical face-selectivity, which on average was approximately 50 mm³ for the fusiform face area, the occipital face area, and the posterior superior temporal sulcus. We suggest that the combination of (a) more robust face-related activity induced by a dynamic face localizer and (b) a cluster-size determination based on maximum face-selectivity increases both the sensitivity and the specificity of the characterization of face-related ROIs in individual subjects. *Hum Brain Mapp* 30:1637–1651, 2009. © 2008 Wiley-Liss, Inc.

Key words: FFA; STS; OFA; functional localizer; fMRI; face processing



[†]Christopher J. Fox and Giuseppe Iaria contributed equally to this study.

Contract grant sponsor: NIMH; Contract grant number: RO1-MH069898; Contract grant sponsor: CIHR; Contract grant number: MOP-77615.

*Correspondence to: Christopher J. Fox, Human Vision and Eye Movement Laboratory, VGH Eye Care Centre - Section D, 2550 Willow Street, Vancouver, BC, Canada V5Z 3N9.

E-mail: cjfox@interchange.ubc.ca

Received for publication 3 March 2008; Revised 16 May 2008; Accepted 29 May 2008

DOI: 10.1002/hbm.20630

Published online 25 July 2008 in Wiley InterScience (www.interscience.wiley.com).

INTRODUCTION

Functional magnetic resonance imaging (fMRI) studies have identified a network of cortical regions that are involved in face perception. The first face-selective region found was the fusiform face area (FFA), located in the right fusiform gyrus [Kanwisher et al., 1997], consistent with the predominance of right inferotemporal lesions in prosopagnosia [Damasio, 1985; de Renzi, 1986; Landis et al., 1986; Meadows, 1974]. Subsequently, other studies have characterized face-selective regions in the inferior occipital gyrus (occipital face area, OFA) and the posterior superior temporal sulcus (pSTS) [Ishai et al., 2005; Rossion et al., 2003; Winston et al., 2004]. Together, these three

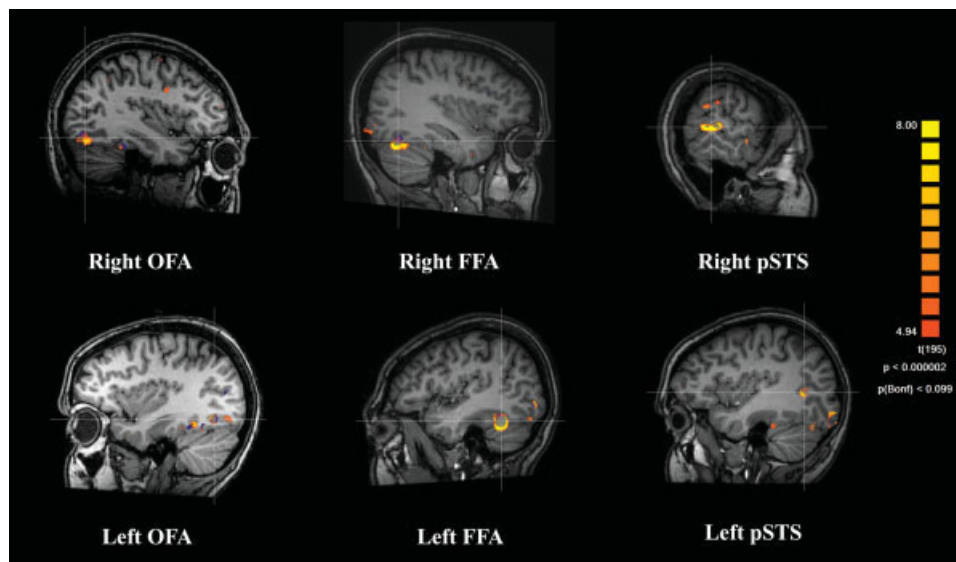


Figure 1.

Representative fMRI images for regions comprising the core system of face perception: occipital face area (OFA); fusiform face area (FFA); posterior superior temporal sulcus (pSTS). Overlay maps of the face > object contrast are set at the threshold of $P < 0.05$ (1-tailed Bonferroni). Results from the *static localizer* are

overlaid in blue and the results of the *dynamic localizer* in orange–yellow. Clear overlaps in all regions can be seen, with more widespread activity readily apparent in the *dynamic localizer* maps. [Color figure can be viewed in the online issue, which is available at www.interscience.wiley.com.]

regions are currently considered the “core system” for face processing [Gobbini and Haxby, 2007; Haxby et al., 2000] (see Fig. 1).

Beyond the core system are a number of additional regions that may contribute to face perception. These include regions in the inferior frontal gyrus (IFG) [Ishai et al., 2005], amygdala (AMG) [Adolphs et al., 1994], precuneus [Kosaka et al., 2003], anterior paracingulate gyrus [Gobbini and Haxby, 2006] and a more anterior portion of the STS [Winston et al., 2004], among others. These regions comprise the “extended system” for face perception [Gobbini and Haxby, 2007; Haxby et al., 2000] (see Fig. 2).

The identification of face-related cortical regions has led to the question of what roles each of these regions may play in face perception [Haxby et al., 2000]. One way to examine the function of these face-related regions is by first identifying or “localizing” the region-of-interest (ROI) and then studying functional changes within this “localized” ROI on subsequent experimental tasks [Saxe et al., 2006; but see Friston et al., 2006]. Functional face localizers today are very similar to the scans used by Kanwisher et al. [1997] who first identified the FFA. These localizers normally contrast hemodynamic activity during blocks in which subjects view static images of faces with blocks of diverse objects, scrambled faces, or a single non-face object class, such as houses [Andrews and Ewbank, 2004; Eger et al., 2004; Gauthier et al., 2000; Golarai et al., 2007; Golby et al., 2001; Ishai et al., 2000, 2005; Mazard et al., 2006; Pyles et al., 2007; Rotshtein et al., 2005; Schiltz

and Rossion, 2006; Yovel and Kanwisher, 2005]. As noted by Kanwisher et al. [1997], and illustrated by these other studies, a contrast between static images of faces and objects does quite well at identifying the right FFA but is not as reliable in identifying the right OFA, right STS, or the left hemispheric counterparts of these three regions. Furthermore, as face-specificity decreases in regions of the extended system, the power of the standard face localizer also decreases [Ishai et al., 2005], making it difficult to identify regions consistently across subjects, and thereby limiting the feasibility of examining specific hypotheses within many of these regions.

One approach to dealing with this problem of inconsistent functional localization is by performing group analyses on normalized brains [Friston et al., 2006; Kosaka et al., 2003; Winston et al., 2004]. Group analyses can identify cortical ROIs in the group data that are not seen consistently in each individual subject. However, normalizations often fail to fully account for between-subject structural anatomic variability [McKeown and Hanlon, 2004; Nieto-Castanon et al., 2003], and even if they did, the group analysis would still be complicated by between-subject functional anatomic variability, in that functionally active regions may vary in their cerebral location from one subject to another [Wohlschlagel et al., 2005].

A second approach to dealing with inconsistent functional localization that avoids normalization has been to vary the statistical threshold at which a ROI is identified in single subjects. Thresholds used in prior studies have

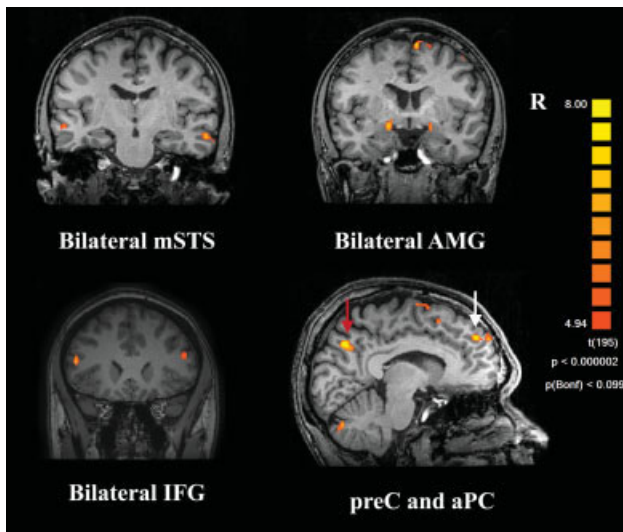


Figure 2.

Representative fMRI images for regions comprising the extended system of face perception. Top left: bilateral middle superior temporal sulcus (mSTS). Top right: bilateral Amygdala (AMG). Bottom Left: bilateral inferior frontal gyrus (IFG). Bottom right: precuneus (preC; red arrow) and anterior paracingulate cortex (aPC; white arrow). Because of the poor localization of these regions using the *static localizer*, overlaid maps are results from the statistical analysis of the *dynamic localizer* (faces > objects; $P < 0.05$, 1-tailed Bonferroni). [Color figure can be viewed in the online issue, which is available at www.interscience.wiley.com.]

ranged from very conservative (e.g., “ $P < 0.05$ with Bonferroni correction for multiple comparisons” [Andrews and Ewbank, 2004; Eger et al., 2004; Schiltz and Rossion, 2006; Schiltz et al., 2006; Sorger et al., 2007]) to more liberal ones (e.g. “ $P < 0.001$ uncorrected” [Golarai et al., 2007; Ishai et al., 2005] or “ $t > 2.0$ uncorrected” [Golby et al., 2001]). More liberal thresholds may reveal more areas more consistently, but do not account for the problem of multiple comparisons across the thousands of voxels within the brain, and are often not objectively set, raising questions about their statistical validity [Genovese et al., 2002]. Furthermore, these variations in threshold can affect not only the likelihood of identifying a functional region, but the size of the functionally activated region. More liberal thresholds tend to show larger areas of activation, and more conservative ones show smaller areas. Which of these thresholds more accurately reflects the anatomic reality is open to question, especially in situations where there are no guiding estimates of the size of a cortical region from primate neurophysiology or human histology.

The inconsistent detection of face-selective areas with current localizer protocols is also problematic for another field, the application of functional imaging to neuropsychological patients. Increasingly fMRI is being used to determine if lesions have affected specific functional regions in specific individuals [Avidan et al., 2005; Rossion et al., 2003]. This is

particularly the case in patients with acquired lesions, where the variability in lesion anatomy makes group analyses inadvisable [Barton, 2003]. However, it is difficult to make firm conclusions if these areas cannot be consistently demonstrated in all healthy individuals.

In the present study, we addressed two issues regarding the localization of face-processing areas in the human brain. First, we asked whether it is possible to create a better face-localizer. Standard functional localizers for face processing rely on a contrast between static images of faces and objects. However, normal experience with these stimuli is dynamic, not static. Also, there is some evidence of increased activity within face-related ROIs for dynamic faces as compared to static faces [Avidan et al., 2005; Kilts et al., 2003; Sato et al., 2004]. Furthermore, neurophysiological studies show that there are neurons that respond to different facial images (e.g., viewpoint differences [Perrett et al., 1991]), which may suggest that the changes in facial image inherent to dynamic stimuli may cause activation of a greater pool of neurons. For these reasons, we hypothesized that the dynamic localizer would result in (1) a higher likelihood of localizing face-processing areas in individual subjects and (2) more robust activity within all face-related ROIs. To study this we compared two functional localizers, one contrasting static images of faces versus objects and the other contrasting dynamic video clips of faces versus objects.

Second, we asked, how large should a face-selective ROI be? Although face-selective responses have been identified within the inferotemporal cortex and STS in monkeys [Perrett et al., 1982], there is no neurophysiologically based estimate of size for any potential homologues of the FFA, OFA, or STS (unlike the case with the V5 complex [Brewer et al., 2002]). In the absence of such anatomic data, we asked whether it would be possible to derive statistical criteria that would provide more consistent estimates of the size of face-selective regions, with optimum specificity for face stimuli.

DEFINING FACE-SELECTIVE ROIs: LOCALIZERS WITH STATIC OR DYNAMIC STIMULI

Materials and Methods

Participants

Sixteen right-handed healthy participants (Eight females; Mean age \pm SD: 25.6 \pm 4.1 years) with normal or corrected-to-normal vision and no history of neurological disorders participated. Informed consent was obtained and the protocol approved by the institutional review boards of the University of British Columbia and Vancouver General Hospital, in accordance with The Code of Ethics of the World Medical Association, Declaration of Helsinki [Rickham, 1964].

TABLE I. Objects included in the dynamic localizer and associated within-object motions

Fountain spraying	Piano keys depressing
Ceiling fan spinning	Plant blowing
Globe spinning	Record player rotating
Merry-go-round rotating	Roulette wheel spinning
Jiffy-pop expanding	Scale balancing
Juice pouring	Scale needle rotating
Kettle steaming	Oscilloscope wave fluctuating
Tree branch blowing	Stopwatch numbers changing
Newton's balls bouncing	Tennis ball spinning
Gears cranking	Car tire rotating
Toilet water flushing	Coffee machine pouring
Top spinning	Film reels rotating
Traffic light changing	Grass and heather blowing
Office fan oscillating	Waterfall flowing
Washing machine spinning	Fireplace burning
Water faucet dripping	Fireworks exploding
Windmill rotating	Flag waving
Blender mixing	Eggs and water boiling
Candle flickering	Flower blowing
Cigarette burning	Sewing machine sewing

Stimuli

Participants underwent two functional scans. During the first functional scan participants viewed static photographs of nonliving objects (e.g., television, basketball) and faces (neutral and expressive) presented in separate blocks. This *static localizer* is similar to those used to identify face-related cerebral regions by Kanwisher et al. [1997] and others [Andrews and Ewbank, 2004; Golarai et al., 2007; Golby et al., 2001; Grill-Spector et al., 2004; Mazard et al., 2006; Pyles et al., 2007; Reddy and Kanwisher, 2007; Rhodes et al., 2004; Schiltz et al., 2006; Schwarzlose et al., 2005; Sorger et al., 2007; Spiridon and Kanwisher, 2002; Yovel and Kanwisher, 2005]. Participants performed a “one-back task,” that is, to press a button if an image was identical to the previous one. The *static localizer* began and ended with a fixation block showing a cross in the center of an otherwise blank screen. Additional fixation blocks were alternated with image blocks, with all blocks lasting 12 s. Six blocks of each image category (object, neutral face, expressive face) were presented in a counterbalanced order. Each image block consisted of 15 images (12 novel and three repeated), all sized to a width of 400 pixels and presented at screen center for 500 ms, with an interstimulus-interval of 300 ms. The *static localizer* took 444 s in total.

During the second functional scan, participants viewed video-clips of nonliving objects and faces presented in separate blocks. We referred to this scan as the *dynamic localizer*. Video-clips of faces all displayed dynamic changes in facial expression (i.e., from neutral to happy). So that dynamic changes in objects were comparable with those seen in faces, all video-clips of objects displayed types of motion that did not create large translations in position (see Table I). Participants again performed a one-back task. Identical fixation blocks began and ended the session and were alternated with image blocks, with all blocks lasting

12 s. Eight blocks of each image category (object, face) were presented in a counterbalanced order. Each image block consisted of six video-clips (five novel and one repeated) presented centrally for 2,000 ms each. Video-clips of objects were gathered from the Internet, and video-clips of faces were provided by Chris Benton (Department of Experimental Psychology, University of Bristol, UK) [Benton et al., 2007]. All video-clips were resized to a width of 400 pixels. The *dynamic localizer* took 396 s in total. (The *dynamic localizer* is available by contacting the corresponding author.)

fMRI data acquisition and analysis

All scans were acquired in a 3.0 Tesla Philips scanner. Stimuli were presented using Presentation 9.81 software and were rear-projected onto a mirror mounted on the head coil. Whole brain anatomical scans were acquired using a T1-weighted echoplanar imaging sequence, consisting of 170 axial slices of 1 mm thickness (1 mm gap) with an in-plane resolution of 1 mm × 1 mm (FOV = 256). T2-weighted functional scans (TR = 2 s; TE = 30 ms) were acquired using an interleaved ascending echoplanar imaging sequence, consisting of 36 axial slices of 3 mm thickness (1 mm gap) with an in-plane resolution of 1.875 mm × 1.875 mm (FOV = 240). The *static localizer* scan consisted of 223 functional volumes, whereas the *dynamic localizer* scan consisted of 199 functional volumes.

The first volume of each functional scan was discarded to allow for scanner equilibration. All MRI data were analyzed using BrainVoyager QX Version 1.8 (www.brainvoyager.com). Anatomical scans were not preprocessed. Preprocessing of functional scans consisted of corrections for slice scan time acquisition, head motion (trilinear interpolation), and temporal filtering with a high pass filter to remove frequencies less than three cycles/time course. For each participant, functional scans were individually coregistered to their respective anatomical scan, using the first retained functional volume to generate the coregistration matrix, and were resliced (1 mm³) to match the anatomical scan.

The *static localizer* time course was analyzed with a single subject general linear model (GLM), with object (O), neutral (NF), and expressive (EF) faces as predictors. Analysis of NF + EF > 2*O was overlaid on the whole brain and significance was set at $P < 0.05$, with correction for multiple comparisons (1-tailed Bonferroni). A similar procedure was adopted for the *dynamic localizer*, the time course of which was analyzed via a single subject GLM with objects (O) and faces (F) as predictors. Analysis of F > O was overlaid on the whole brain and significance was set at $P < 0.05$, with correction for multiple comparisons (1-tailed Bonferroni).

ROI localization and analysis

Within each participant, we first attempted to define each of the three face-related regions comprising the core

system of face perception. Face-related voxels located on the lateral temporal portion of the fusiform gyrus were designated as the FFA, whereas voxels located on the lateral surface of the inferior occipital gyrus were designated as the OFA. Face-related voxels located on the posterior segment of the STS were designated as the pSTS. All regions were defined in both right and left hemispheres.

In addition to these “core” face-processing regions, we also examined regions comprising the extended system of face perception. Face-related voxels located on the anterior segment of the superior temporal sulcus of the right or left hemispheres were designated as the middle superior temporal sulcus (mSTS) as described by Winston et al. [2004]. Face-related voxels within the AMG and IFG were identified bilaterally. Face-related voxels within the precuneus (preC) and the anterior paracingulate cortex (aPC) were defined without lateralization because of their location at the midline between cerebral hemispheres.

For each identified ROI, the t -value of the peak voxel and cluster size (number of voxels) was determined. ROIs that were not identified at the *a priori* statistical threshold ($P < 0.05$, 1-tailed Bonferroni) were assigned a cluster size of zero, but the statistical threshold was lowered to a more liberal False-Discovery-Rate threshold of $q < 0.05$ (corrected for multiple comparisons) to determine the t -value of the peak voxel within that region. For statistical analysis, failing to localize a region at the False-Discovery-Rate threshold resulted in this region being assigned the False-Discovery-Rate threshold as a default t -value of its peak voxel.

Analyses were performed separately for the core and extended systems. An initial paired t -test was performed within each system, with the number of ROIs localized within each subject as the dependent variable, to deter-

mine whether one localizer more consistently localized face-related ROIs than the other. All core system GLM consisted of localizer (*static*, *dynamic*), ROI (OFA, FFA, pSTS), and hemisphere (right, left) as fixed factors and subject as a random factor. The unilateral nature of the precuneus and aPC made it impossible to include hemisphere as a factor, thereby restricting all extended system GLMs to localizer (*static*, *dynamic*) and ROI (right-mSTS, left-mSTS, right-AMG, left-AMG, right-IFG, left-IFG, preC, aPC) as fixed factors and subject as a random factor. Within each system, five separate univariate GLMs were performed, each with a different dependent variable: (i) t -value of the peak voxel; (ii) cluster size; (iii) X Talairach coordinate of the peak voxel; (iv) Y Talairach coordinate peak voxel; and (v) Z Talairach coordinate of the peak voxel. GLMs considering t -value of the peak voxel and cluster size assessed the robustness and extent of face-related activity respectively. GLMs considering Talairach coordinates of the peak voxel determined whether both the *static* and *dynamic* localizers did in fact localize the same functional regions. Post-hoc t -tests were performed to analyze all significant effects. All statistical analyses were performed using SPSS 14.0 (www.spss.com), and significance on all tests was set at $\alpha < 0.05$.

Results

Core system

When localizing ROIs comprising the core system of face perception, the *static localizer* operated at a 72% success rate, whereas the *dynamic localizer* achieved a 98% success rate, a statistically significant difference [$t(15) = -3.93$; $P = 0.001$]. The *dynamic localizer* was more successful than the *static localizer* in localizing all regions of the

TABLE II. Core system of face perception

Region-of-interest (Core system)	Localizer	# of subjects ($n = 16$)	X	Y	Z
Right OFA	Static	10	40 ± 11	-75 ± 20	-9 ± 8
	Dynamic	16	36 ± 10	-79 ± 19	-14 ± 8
Left OFA	Static	14	-38 ± 10	-73 ± 19	-15 ± 8
	Dynamic	15	-37 ± 10	-74 ± 19	-17 ± 7
Right FFA	Static	13	35 ± 9	-48 ± 14	-19 ± 7
	Dynamic	16	37 ± 9	-48 ± 15	-20 ± 7
Left FFA	Static	16	-35 ± 10	-42 ± 12	-20 ± 6
	Dynamic	16	-37 ± 9	-43 ± 13	-20 ± 6
Right pSTS	Static	11	53 ± 13	-44 ± 13	4 ± 5
	Dynamic	16	54 ± 13	-41 ± 13	4 ± 5
Left pSTS	Static	5	-50 ± 14	-55 ± 16	8 ± 5
	Dynamic	15	-51 ± 14	-52 ± 15	6 ± 5

Number of participants in whom the ROI was localized and average Talairach coordinates (Mean \pm SD) are reported for both the static and dynamic localizers. ROIs were localized using the contrast faces > objects with a statistical threshold of $P < 0.05$ (1-tailed Bonferroni). The dynamic localizer was more consistent in identifying face-related ROIs in all areas of the core system excluding the left FFA, which was identified in all subjects with both localizers. Average Talairach coordinates of the peak voxels show that static and dynamic localizers localized similarly positioned ROIs.

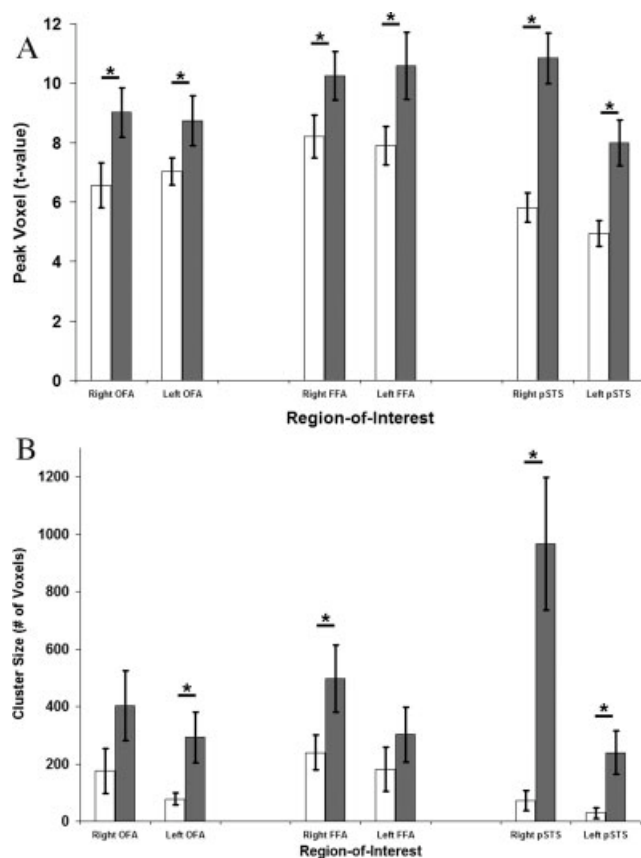


Figure 3.

Results from the statistical comparison of the *static* (white bars) and *dynamic* localizers (gray bars) (Mean ± SEM). **A:** When using the *dynamic* localizer significantly higher *t*-values are seen in the peak voxel of all regions in the core system (indicated with an asterisk), with the largest effects observed in the pSTS. **B:** Use of the *dynamic* localizer results in the localization of significantly larger clusters of face-related activity within the left-OFA, right-FFA, and bilateral-pSTS (indicated with an asterisk), with a similar but nonsignificant pattern observed in other regions of the core system.

core system except the left-FFA, which was localized in all subjects with both localizers (Table II). The only regions not identified with 100% success with the *dynamic* localizer were the left OFA and left pSTS, which were missed in one subject each. In contrast, the *static* localizer had difficulty locating even the right FFA in three subjects. In contrast to our findings with the *static* localizer previous reports have shown more consistent activation in the right than left FFA [Jiang et al., 2006; Kanwisher et al., 1997] suggesting right hemispheric dominance in face processing [Barton, 2003].

Regarding the *t*-value of the peak voxel, we observed a significant main effect of localizer [$F(1,15) = 46.15; P < 0.001$] with the *dynamic* localizer (Mean *t*-value ± SEM; 9.57 ± 0.37) eliciting more robust face-related activity than

the *static* localizer (6.74 ± 0.26) (see Fig. 1). We also observed a main effect of ROI [$F(2,30) = 4.45; P < 0.05$] and an interaction between ROI and Hemisphere [$F(2,30) = 4.15; P < 0.05$], with the strongest face-related activity within the FFA (right = 9.22 ± 0.57 ; left = 9.23 ± 0.68) and the weakest within the left-pSTS (6.47 ± 0.51). Finally, we observed a significant interaction between localizer and ROI [$F(2,30) = 5.41; P = 0.01$], with significantly more robust activity elicited by the *dynamic* localizer in all regions of the core system ($P < 0.001$, all tests), but with the largest effects occurring within the pSTS ($\Delta t\text{-value} \pm \text{SEM}$; OFA = 2.08 ± 0.56 , FFA = 2.35 ± 0.51 , pSTS = 4.03 ± 0.59) (Fig. 3A).

To further examine the effects of the *dynamic* localizer on the observed *t*-value of the peak voxel, we performed correlation analyses between *static* and *dynamic* peak *t*-value within each of the core region ROIs. We observed a significant positive correlation in all regions of the core system ($r > 0.59, P < 0.05$; all tests) except the left pSTS ($r = 0.32$, n.s.). This result suggests that the *dynamic* localizer not only successfully localizes these ROIs in more subjects, but also consistently increases activity within ROIs that were successfully localized with the *static* localizer. Finally, a visual inspection of the averaged response time course for faces and objects, within right hemisphere ROIs of the core system (see Fig. 4), provides more insight into the effects of the *dynamic* localizer by demonstrating both an increased face response (right OFA, pSTS), and a decreased object response (right OFA, FFA).

The analysis of ROI cluster size showed a similar pattern to those observed when considering the *t*-value of the peak voxel. We found main effects of localizer [$F(1,15) = 21.65; P < 0.001$] with larger clusters elicited by the *dynamic* localizer (Mean # of voxels ± SEM; 450 ± 58) than the *static* localizer (129 ± 23) and of hemisphere [$F(1,15) = 16.81; P = 0.001$] with larger clusters in the right hemisphere (392 ± 58) than in the left (187 ± 28). Significant interaction effects between localizer and ROI [$F(2,30) = 4.62; P < 0.05$] and between localizer and hemisphere [$F(1,15) = 13.67; P < 0.005$] were modified by a three-way interaction between localizer, ROI, and hemisphere [$F(2,30) = 5.77; P < 0.01$]. Post-hoc *t*-tests revealed significantly larger clusters elicited by the *dynamic* localizer in the left-OFA, right-FFA, and bilateral-pSTS ($P < 0.05$, all tests) with a trend in the same direction for the right-OFA ($P = 0.06$). Again the largest effect of the *dynamic* localizer was observed in the right-pSTS (Δ cluster size ± SEM = 896 voxels ± 234; Fig. 3B).

Finally, we performed GLMs considering the Talairach coordinates of the peak voxel of all localized ROIs. Although we saw significant main effects of ROI and significant interaction effects between ROI and hemisphere for all three coordinates [$F(2,30) > 5.00; P < 0.05$, all tests], as can be expected for ROIs found in different cortical areas, the only significant effect of localizer was a three-way interaction between localizer, ROI and hemisphere when considering the X (medial-lateral) coordinate [$F(2,24) = 4.283; P <$

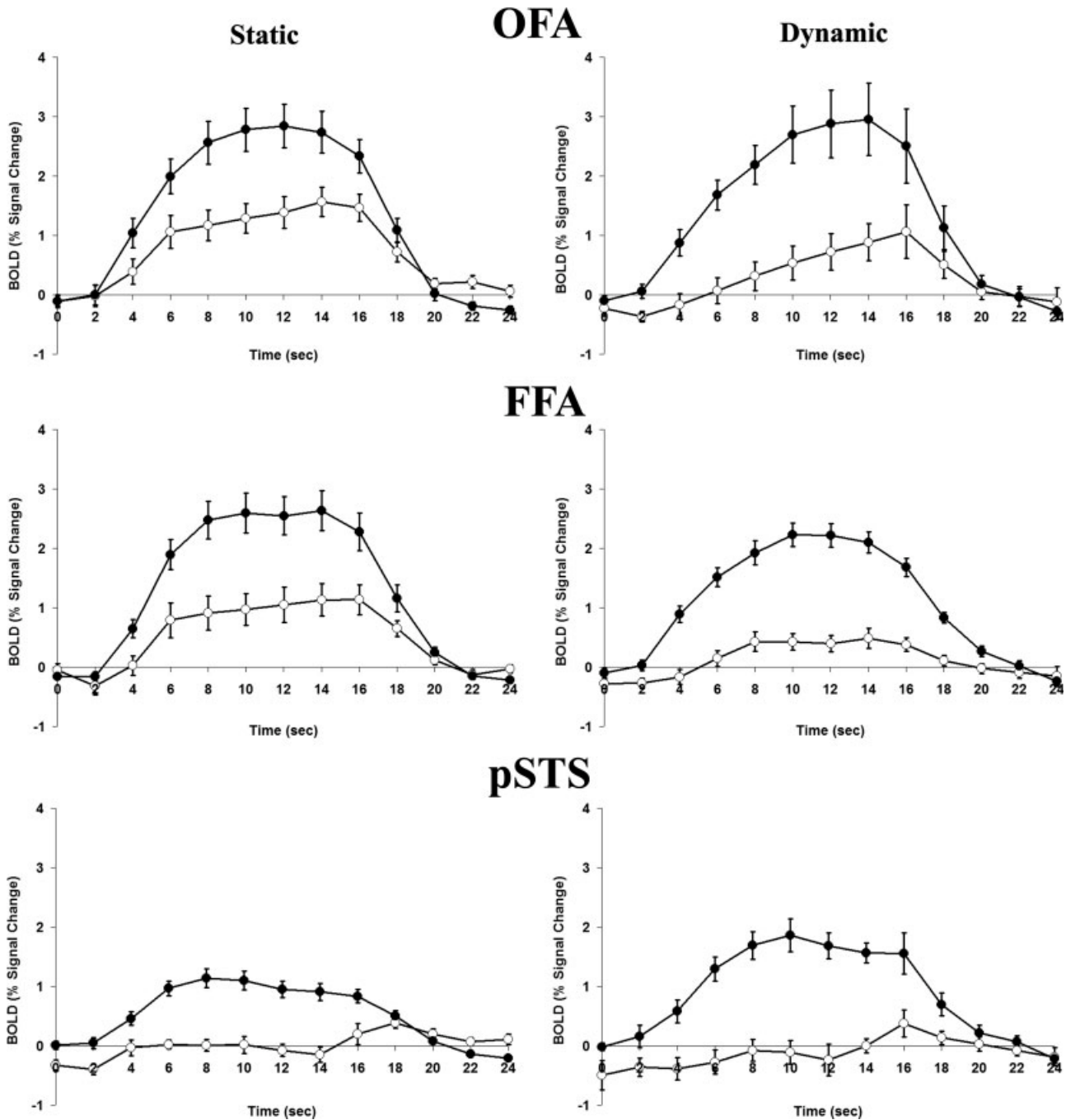


Figure 4.

Response time courses for faces (filled circles) and objects (open circles) within the right OFA (top), right FFA (middle), and right pSTS (bottom). Time courses were extracted from the individually localized ROIs and averaged (Mean \pm SEM).

Responses from the *static localizer* are presented in the left column, and the *dynamic localizer* in the right column. The *dynamic localizer* increases the separation of signal between faces and objects in all three of these core face processing regions.

0.05]. Post-hoc *t*-tests revealed a significant difference in the X coordinate of the right-FFA as localized by the *static* and *dynamic localizers* ($P < 0.05$), with the *static* right-FFA

slightly more medial (Mean X coordinate \pm SEM; 35 ± 1) than the *dynamic* right-FFA (37 ± 1). Although this difference in the X coordinate of the peak voxel of the right FFA

TABLE III. Extended system of face perception

Region-of-interest	Localizer	# of subjects ($n = 16$)	X	Y	Z
Right mSTS	Static	5	51 ± 14	-5 ± 8	-9 ± 6
	Dynamic	11	49 ± 12	-5 ± 10	-11 ± 7
Left mSTS	Static	3	-53 ± 14	-16 ± 8	-5 ± 6
	Dynamic	12	55 ± 15	-16 ± 8	-5 ± 6
Right AMG	Static	3	18 ± 5	-2 ± 2	-13 ± 5
	Dynamic	7	18 ± 6	-4 ± 2	-11 ± 4
Left AMG	Static	0	18 ± 8	-3 ± 4	-11 ± 5
	Dynamic	5	19 ± 7	-6 ± 4	-14 ± 5
Right IFG	Static	7	42 ± 11	19 ± 10	26 ± 12
	Dynamic	15	46 ± 12	21 ± 11	22 ± 12
Left IFG	Static	6	-40 ± 12	20 ± 11	20 ± 11
	Dynamic	12	-47 ± 12	17 ± 7	21 ± 9
preC	Static	7	0 ± 4	-59 ± 18	30 ± 11
	Dynamic	14	1 ± 4	-62 ± 16	30 ± 10
aPC	Static	9	2 ± 5	59 ± 15	7 ± 9
	Dynamic	12	6 ± 4	54 ± 14	20 ± 12

Number of participants in whom the ROI was localized and average Talairach coordinates (Mean ± SD) are reported for both static and dynamic localizers. ROIs were localized using the contrast faces > objects with a statistical threshold of $P < 0.05$ (1-tailed Bonferroni). In all cases, the dynamic localizer was more consistent in identifying face-related ROIs. Average Talairach coordinates of the peak voxels show that static and dynamic localizers localized similarly positioned ROIs.

is statistically significant, the absolute difference (2 mm) becomes negligible when considering the mean volume of the right-FFA (368 mm³). Thus both the *static* and *dynamic localizers* appear to be localizing the same regions of face-related activity (Table II; Fig. 1).

Extended system

Although the *static localizer* only found 31% of regions in the extended system, the *dynamic localizer* had a 69% success rate, a significant difference [$t(15) = -4.24$; $P = 0.001$]. The *dynamic localizer* was more successful in localizing all regions of the extended system (Table III; Fig. 2).

Regarding the t -value of the peak voxel, we observed a significant main effect of localizer [$F(1,15) = 19.18$; $P = 0.001$] with the *dynamic localizer* (Mean t -value ± SEM; $6.12 ± 0.18$) eliciting more robust face-related activity than the *static localizer* ($4.45 ± 0.10$). We also observed a main effect of ROI [$F(7,105) = 6.99$; $P < 0.001$] with the strongest face-related activity within the right-IFG ($6.19 ± 0.39$) and the weakest within the AMG (right = $4.57 ± 0.24$; left = $4.12 ± 0.22$). Finally, we observed a significant interaction between localizer and ROI [$F(7,105) = 2.55$; $P < 0.05$], with significantly more robust activity elicited by the *dynamic localizer* in all regions of the extended system ($P < 0.05$, all tests) except the left-IFG, which showed a trend in the same direction ($P = 0.053$) (Fig. 5A).

Analysis of ROI cluster size showed a similar pattern. We observed a significant main effect of localizer [$F(1,15) = 12.07$; $P < 0.005$] with larger clusters elicited by the *dynamic localizer* (Mean # of voxels ± SEM; $189 ± 36$) than

by the *static localizer* ($13 ± 4$). We also observed a main effect of ROI [$F(7,105) = 3.28$; $P < 0.005$] with the largest clusters observed within the right-IFG ($218 ± 76$) and the smallest within the AMG (right = $13 ± 6$; left = $11 ± 6$). Finally, we observed a significant interaction between localizer and ROI [$F(7,105) = 3.14$; $P < 0.01$], with significantly larger clusters elicited by the *dynamic localizer* in the bilateral mSTS, right-IFG, precuneus, and anterior paracingulate ($P < 0.05$, all tests) (Fig. 5B).

Finally, a comparison of Talairach coordinates of the peak voxel for all localized ROIs revealed main effects of ROI for all three coordinates [$F(7,105) > 100$; $P < 0.001$, all tests], as can be expected for ROIs located in different cortical areas, and significant interaction effects between localizer and ROI for the X coordinate [$F(7,79) = 3.89$; $P = 0.001$] and the Z (superior-inferior) coordinate [$F(7,79) = 3.035$; $P < 0.01$], but not the Y (anterior-posterior) coordinate [$F(7,79) = 0.30$; $P > 0.50$]. Post-hoc t -tests revealed a significant difference in the X coordinate for the left-IFG ($P < 0.01$), with the *static* left-IFG slightly more medial (Mean coordinate ± SEM; $-40 ± 1$) than the *dynamic* left-IFG ($-47 ± 1$). Differences were also observed in the X coordinate ($P < 0.05$) and the Z coordinate ($P < 0.005$) of the aPC, with the *static* aPC more medial ($2 ± 1$) and inferior ($7 ± 2$) to the *dynamic* aPC (X = $6 ± 1$; Z = $20 ± 3$). Although the absolute differences seen here are larger than those seen within the right-FFA (leftIFG-X = 7 mm; aPC-X = 4 mm; aPC-Z = 13 mm) the differences in peak voxel location are still negligible when compared to the mean volume of these regions (left-IFG = 40 mm³; aPC = 184 mm³). Thus, with the possible exception of the left-IFG and the aPC, both the *static* and *dynamic localizers*

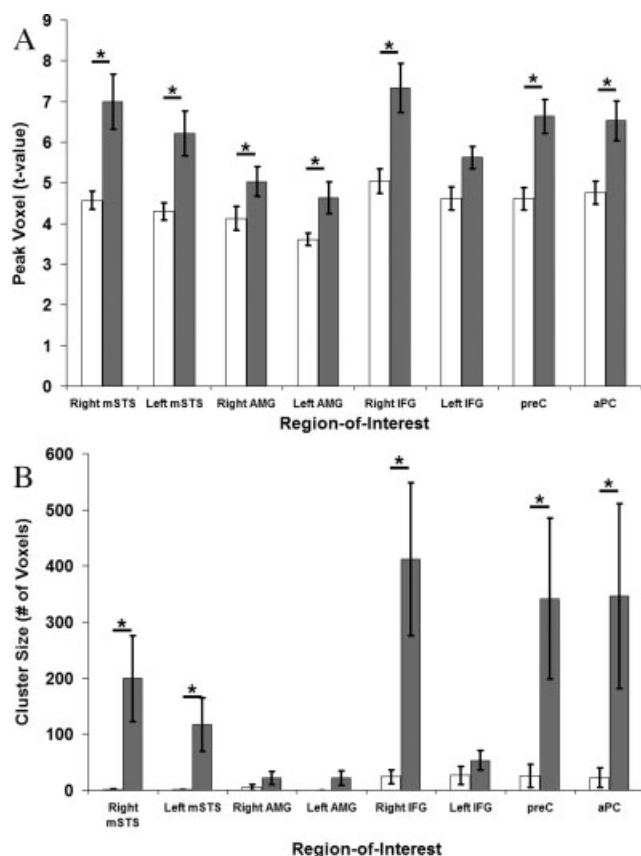


Figure 5.

Results from the statistical comparison of the *static* (white bars) and *dynamic localizers* (gray bars) (Mean \pm SEM). **A:** When using the *dynamic localizer* significantly higher *t*-values are seen in the peak voxel of all regions in the extended system (indicated with an asterisk), excluding the left-IFG, which shows a trend in the same direction. **B:** Use of the *dynamic localizer* results in the localization of significantly larger clusters of face-related activity within the bilateral mSTS, right-IFG, preC, and aPC (indicated with an asterisk).

appear to be localizing the same regions of face-related activity (Table III; Fig. 2).

DEFINING FACE-SELECTIVE ROIs: THE STATISTICALLY OPTIMAL CLUSTER SIZE

The *dynamic localizer* proved to be a much more consistent localizer of face-related activity than the *static localizer*, for both the core and extended systems of face perception. As well, we found increases in the cluster size of many face-related ROIs. This increase in cluster size highlights an additional question regarding functional localization: what is the “right size” of the cortical region being identified?

This problem of variable cluster size is not unique to our contrast between static and dynamic localizers. Variations in the statistical threshold used to define face-selective activation in the literature have resulted in a wide range of reported cluster sizes for all regions of the core system: right-OFA, 138 mm³ [Sorger et al., 2007] to 4289 mm³ [Ishai et al., 2004]; left-OFA, 312 mm³ [Schiltz and Rossion, 2006] to 4430 mm³ [Ishai et al., 2004]; right-FFA, 498 mm³ [Schiltz and Rossion, 2006] to 4711 mm³ [Ishai et al., 2004]; left-FFA, 379 mm³ [Schiltz and Rossion, 2006] to 4500 mm³ [Ishai et al., 2004]; right-pSTS, 193 mm³ [Sorger et al., 2007] to 5695 mm³ [Ishai et al., 2004]; and left-pSTS, 156 mm³ [Sorger et al., 2007] to 3656 mm³ [Ishai et al., 2004]. Indeed, even within the regions we localized in the present study we see individual clusters identified as the right-FFA up to a volume of 766 mm³ when using the *static localizer* and up to a volume of 1657 mm³ when using the *dynamic localizer*.

The 10-fold or greater variation in ROI size reported in the face-processing literature underscores the problem of threshold-dependent methods of defining ROI size. Although there may be some intersubject variability in ROI size, these estimates can also vary within individuals when signal strength is modulated by additional factors such as attention and fatigue [Wojciulik et al., 1998]. However, adjusting findings to approximate the “right size” of these functional areas is impossible without additional data from other sources on the anatomic size of these regions. In the absence of such information, asking what should be the “right size” of an ROI becomes a question of what is the statistically optimal estimate of ROI size.

In this direction, some efforts have been made to determine the “right size” of localized ROIs using complex statistical techniques [Ng et al., 2007], and others have noted that face-selectivity decreases with increased ROI size [Golarai et al., 2007]. Although not directly assessing the “right size” of localized ROIs, other groups have combined a functional localizer with experimental scans to increase the “selectivity” of ROIs used for subsequent experimental analyses [Yovel and Kanwisher, 2005]. Within any given ROI is a peak voxel that shows the largest difference between face-related activity and object-related activity (face > object). With the statistical threshold set to this maximal difference we observe a cluster of only 1 voxel in size. As the threshold is reduced to include more voxels in the cluster the average face > object difference will decrease (all other voxels have a smaller face > object difference than the peak voxel), but the standard deviation of this average difference will also decrease (due to the averaging of more and more voxels). Initially, the decrease in standard deviation may result in a larger statistical face > object difference for the cluster, but at some point the decrease in absolute face > object difference of the less selective voxels being added to the cluster will outweigh any further reduction in the standard deviation.

Using this statistical rationale, we attempted to determine at what ROI size the maximal face > object differ-

ence is achieved and thereby estimate the “statistically optimal size” of these face-related ROIs. Because of the wide variety of inputs that can activate ROIs in the extended system (i.e., nonface or nonvisual stimuli), we restricted our analyses to ROIs in the core system which preferentially respond to viewed faces [Haxby et al., 2000].

Materials and Methods

Regions-of-interest and analysis

Participants, stimuli, fMRI data acquisition, fMRI data processing and analyses, and ROI localization were provided in the previous section. Our findings indicated that *static* and *dynamic localizers* did in fact localize the same ROIs within the core system, and that the *dynamic localizer* was more successful in localizing face-related ROIs. For these reasons, only *dynamically localized* ROIs were included in the following analyses. The ROIs which were not localized (2 of 96) at the statistical threshold previously used ($P < 0.05$, 1-tailed Bonferroni) were localized at a more liberal threshold of $q < 0.05$ (False Discovery Rate, corrected for multiple comparisons). This resulted in a full localization of all six core system ROIs in each of the 16 participants.

A single subject GLM (as described in the previous section) was used to estimate the β -weights for faces and objects within the peak voxel of each localized ROI. A t -value for this peak voxel was then calculated using the following formula:

$$t = (\beta_F - \beta_O) / \{\sqrt{[(SD_F)^2 + (SD_O)^2] / n}\} \quad (1)$$

where β_F and β_O represent the predicted β -weights for the face and object conditions, respectively, SD_F and SD_O represent the standard deviation for the predicted face and object β -weights, respectively, and n represents the number of blocks for each condition (eight in the case of the *dynamic localizer*). This calculated t -value will subsequently be referred to as face-selectivity. Face-selectivity was then determined for larger and larger clusters, in 25 voxel increments, which remained centered about their respective peak voxel. For each ROI, when the cluster reached a maximum size of 500 voxels, or when it merged with another cluster of > 25 voxels the process of determining face-selectivity at increasing cluster sizes was stopped.

A group analysis of face-selectivity as a function of cluster size was performed. Change in face-selectivity with respect to the peak voxel was used as the dependent variable rather than absolute face-selectivity (i.e. $t\text{-value}_{(\text{cluster})} - t\text{-value}_{(\text{peak voxel})}$), to account for between-subject variability in this measure. A GLM was performed on these values with ROI (OFA, FFA, pSTS), hemisphere (right, left) and cluster size (1, 25, 50, ..., 450, 475, 500) as fixed factors. Post-hoc t -tests were performed on all significant main and interaction effects. Of particular interest for this analysis is a main effect of cluster size, which would indicate differing

levels of face-selectivity in clusters of different sizes. Post-hoc t -tests would then indicate at what cluster sizes we observed an increase in face-selectivity over that of the peak voxel alone, allowing for an estimate of the statistically optimal size of the ROI.

Next, an individual-based analysis was performed by determining the cluster size at which maximal face-selectivity was observed for each ROI in each individual. A priori 1-tailed t -tests were performed separately on each of the six core system ROIs to determine whether the average cluster size at which maximal face-selectivity was observed was significantly larger than 1 (i.e., the peak voxel alone). Cluster size was then entered as the dependent variable in a GLM with ROI (OFA, FFA, pSTS) and hemisphere (right, left) as fixed factors and subject as a random factor to determine whether the average cluster size for the maximal face-selectivity differed across ROIs or across hemispheres. Post-hoc t -tests were performed on all significant main and interaction effects.

Finally, as a practical comparison between all three methods of localization we performed a third GLM, with ROI (OFA, FFA, pSTS), hemisphere (right, left) and method (*fixed statistical threshold* as in the first section of this report, *fixed cluster size* using the sizes determined in the group portion of the analysis above, and *individually determined cluster size* using the technique in the last paragraph) as fixed factors, subject as a random factor, and face-selectivity (t -value) as the dependent variable. Post-hoc t -tests were performed on all significant main and interaction effects. Significance levels were set at $\alpha < 0.05$ on all statistical tests.

Results

The initial group analysis revealed a main effect of cluster size [$F(20,1322) = 4.42$; $P < 0.001$]. Post-hoc t -tests comparing the face-selectivity of each cluster size with that of the peak voxel revealed significantly increased face-selectivity in clusters of 25 ($P < 0.001$), 50 ($P < 0.005$), and 75 voxels ($P < 0.05$), with respect to the peak voxel. Significant decreases in face-selectivity were observed for clusters larger than 325 voxels ($P < 0.05$, all tests) with a trend in the same direction for clusters of 300 voxels ($P = 0.06$) (Fig. 6A). Cluster size did not interact significantly with any other factor ($P > 0.50$), indicating a similar pattern of face-selectivity effects within all ROIs (Fig. 6B). However, we did observe a significant interaction between ROI and hemisphere [$F(2,1322) = 5.81$; $P < 0.005$]. Post-hoc t -tests revealed higher face-selectivity on the whole within the right-FFA (Mean \pm SEM; 0.09 ± 0.08) than in any other region ($P < 0.05$, all tests), a result most likely due to the broader peak of increased face-selectivity seen within this ROI (Fig. 6B).

The analysis of the individually determined cluster sizes at which maximal face-selectivity occurs revealed no main effect of ROI or hemisphere or an interaction between the two factors ($P > 0.50$, all tests). This result is in agreement

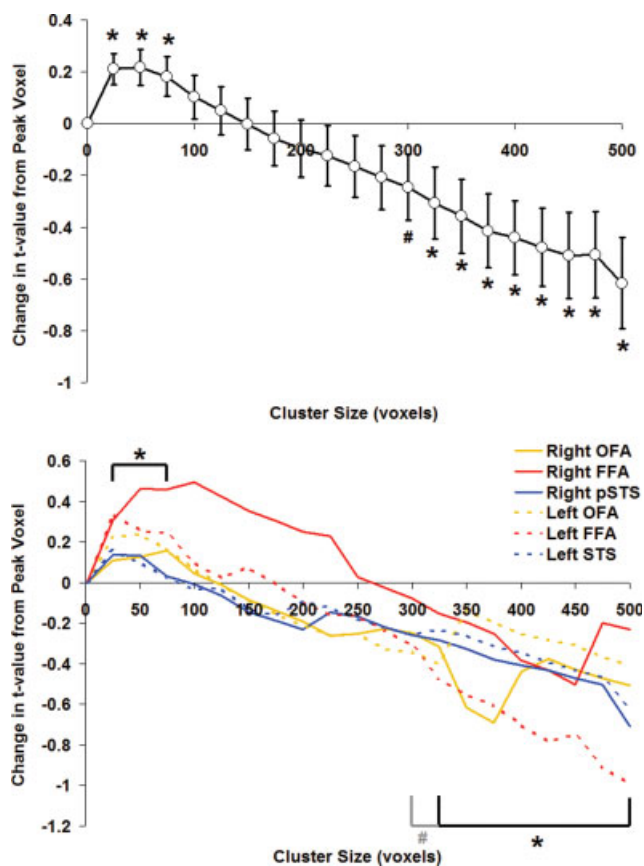


Figure 6.

Face-selectivity as a function of cluster size (Mean \pm SEM; significant values marked with an asterisk and trends with a pound sign). **A:** Averaged results from all six ROIs (bilateral OFA, FFA, and pSTS). Clusters between 25 and 75 voxels show significantly increased face-selectivity with respect to their respective peak voxel. Clusters of > 325 voxels show significantly decreased face-selectivity. **B:** To illustrate the common effect within all six ROIs, individual curves are plotted. A slight broadening of the right-FFA peak of face-selectivity can be observed (solid red line). [Color figure can be viewed in the online issue, which is available at www.interscience.wiley.com.]

with the GLM on the group-determined cluster size of maximal face-selectivity, which showed similar patterns in all six core system ROIs. An average cluster size of roughly 50 voxels (50 mm³) was the size at which maximal face-selectivity was achieved in all ROIs, and a priori *t*-tests showed that this average cluster size was in fact significantly larger than 1 (i.e., the peak voxel alone), again for all 6 ROIs ($P < 0.05$) (Fig. 7A). A frequency plot of the individually determined cluster size with maximal face-selectivity reveals a skewed distribution with most ROIs reaching maximal face selectivity by a cluster size of 75 voxels (83.33%) and only two of 96 ROIs (2.08%) reaching maximal face-selectivity in clusters larger than 200 voxels (Fig. 7B).

Finally, in the direct comparison of methods of localization, we observed a main effect of ROI [$F(2,30) = 4.97$; $P < 0.05$] and an interaction between ROI and Hemisphere [$F(2,30) = 4.56$; $P < 0.05$], indicating differing levels of face-selectivity (*t*-value) across the core system ROIs. Of particular interest was a main effect of localization method [$F(2,30) = 12.51$; $P < 0.01$]. All other main and interaction effects were not significant. Post-hoc analysis of the main effect of localization method revealed a significant increase in face-selectivity when using a fixed cluster size threshold over using a fixed statistical threshold of $P < 0.05$, 1-tailed Bonferroni ($P < 0.001$), and the method of individually determined optimal cluster size showing greater face-selectivity than the other two methods ($P < 0.001$, both tests) (see Fig. 8). Furthermore, both the ROIs of individually determined cluster size (Mean Δt -value \pm SEM; 0.46 ± 0.06) and the ROIs localized with a fixed cluster size (0.22 ± 0.07) showed higher face-selectivity than the peak voxel alone, whereas ROIs localized using a fixed statistical threshold showed, on average, lower face-selectivity than the peak voxel alone (-0.46 ± 0.13).

DISCUSSION

We investigated a new functional localizer which contrasts dynamic videos of faces and objects rather than static images of faces and objects, as used in standard localizers of face-related activity [Yovel and Kanwisher, 2005]. We showed that this *dynamic localizer* was able to more consistently identify regions comprising the core system of face perception (i.e., OFA, FFA, pSTS, see [Haxby et al., 2000]) than a *static localizer*. In fact, localization of these regions approached 100% efficiency across 16 subjects with the *dynamic localizer*. ROIs localized by the *dynamic localizer* were more robust (higher *t*-value of the peak voxel) and larger (bigger clusters) than those localized by the *static localizer*.

Within the core system, we noted the greatest effects of *dynamic localizer* within the pSTS, a region that has been more difficult to localize than the FFA in prior studies [Andrews and Ewbank, 2004; Kanwisher et al., 1997; Yovel and Kanwisher, 2005]. A number of studies have shown activation by biological motion or dynamic stimuli in the pSTS [Pelphrey et al., 2005; Puce et al., 1998; Puce and Perrett, 2003; Thompson et al., 2007; Wheaton et al., 2004]. The proximity of this region to the V5 complex [Puce et al., 1998] may raise concerns that increased activation was related to motion-selective responses. However, our localizer used moving stimuli in both the face and object displays, whereas motion-selective responsivity is usually defined by a contrast between moving and static stimuli [Puce et al., 1998]. Rather, the increased activation of the pSTS by our dynamic localizer may be related to the proposal that the pSTS is particularly sensitive to the dynamic aspects of a face, such as expression [Haxby et al., 2000].

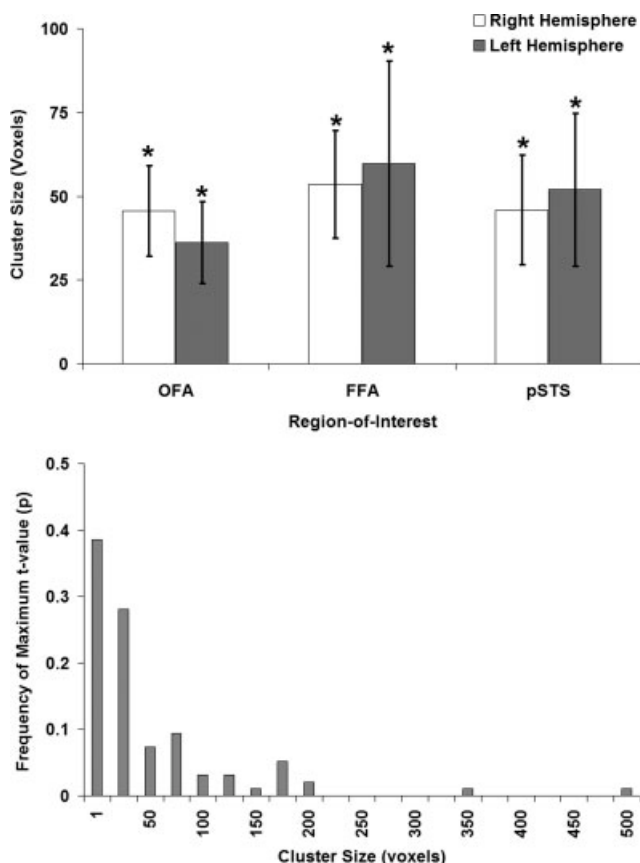


Figure 7.

A: Average cluster size at which maximal face-selectivity is observed (~50 voxels). A GLM indicates no difference between the average cluster size of all six ROIs (bilateral OFA, FFA, and pSTS). All cluster sizes are significantly larger than the peak voxel alone (indicated with an asterisk). **B:** A frequency plot of the cluster size at which maximal face-selectivity is observed reveals the majority of ROIs reaching maximal face selectivity by a cluster size of 75 voxels, with very few requiring clusters of greater than 200 voxels to achieve maximal face-selectivity.

In addition to the improved localization of regions in the core-system, the *dynamic localizer* also improved localization within the extended system of face perception [Haxby et al., 2000], such as the middle superior temporal sulcus [Winston et al., 2004], AMG [Adolphs et al., 1996], IFG [Ishai et al., 2005], precuneus [Kosaka et al., 2003], and aPC [Gobbini and Haxby, 2007]. Because of the inconsistent localization of these regions using standard *static localizers* [Ishai et al., 2005], studies of these areas often rely on group-based analyses within normalized brains [Winston et al., 2004]. The more consistent localization using *dynamic* stimuli may allow these regions to be studied in individual brains.

Why is the *dynamic localizer* so much more consistent in the localization of face-related activity? First, the simple answer may be that dynamic stimuli are more ecologically

valid than static images of faces and objects: empirically, there is evidence that dynamic stimuli activate regions throughout the brain much more strongly than static versions of the same stimuli [Kilts et al., 2003; Sato et al., 2004]. Second, some groups have demonstrated attentional modulations of activity within core regions of the face processing system [Palermo and Rhodes, 2007], and indeed dynamic stimuli may be more attentionally captivating than their static counterparts. However, we explicitly controlled for attentional effects by requiring subjects to perform the same one-back task during *static* and *dynamic localizers*. Furthermore, we ensured that both faces and objects included in the *dynamic localizer* contained dynamic information (Table I), thus equating potential attentional effects associated with dynamic stimuli across these two stimulus classes. Third, since face-selective fMRI responses show adaptation to repeated presentation of the same face, one might ask whether these responses might show rapid adaptation to static faces, which are a single unchanging image, than dynamic faces, which continuously change; however, it is not clear whether adaptation of fMRI signal can occur over the short duration of our images (500 ms), and the long temporal profile of the hemodynamic response makes this somewhat unlikely. Last, even though our static images contained both neutral and expressive faces, the dynamic stimuli by their nature contained a

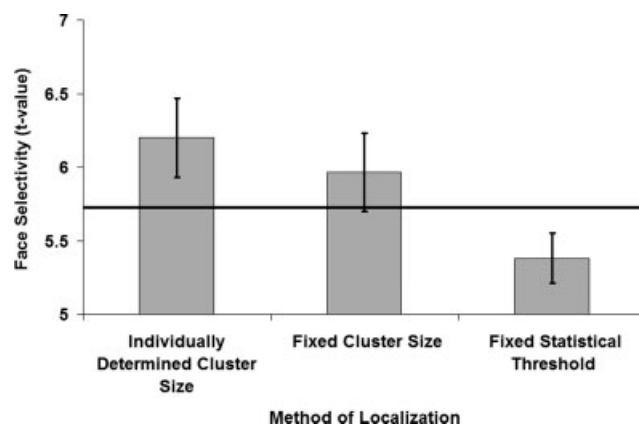


Figure 8.

Face-selectivity comparison of ROIs localized with three different methods (Mean t-value ± SEM). Using a fixed statistical threshold is the least effective method of localizing face-selective ROIs. The use of a fixed cluster size localizes ROI which are more face-selective, but the use of individually based statistics to determine optimal cluster size is the most effective way of ensuring the localization of face-selective ROIs. All differences are significant ($P < 0.001$). The solid bar indicates average face-selectivity of the peak voxel alone. Individually determined cluster size and fixed cluster size methods result in ROIs with face-selectivity greater than the peak voxel alone, whereas a fixed statistical threshold results in ROIs with reduced face-selectivity with respect to the peak voxel.

greater range of facial images. Given the selectivity of some face-responsive neurons to specific views and types of faces [Perrett et al., 1991], this greater range might activate a larger pool of neurons than the static stimuli.

The contrast between the *static* and the *dynamic localizer* also illustrated another issue: variability in ROI cluster size. Many other studies that localize face-selective ROIs employ a fixed statistical threshold [Andrews and Ewbank, 2004; Eger et al., 2004; Gauthier et al., 2000; Golarai et al., 2007; Golby et al., 2001; Ishai et al., 2005, 2000; Kanwisher et al., 1997; Mazard et al., 2006; Pyles et al., 2007; Rotshtein et al., 2005; Schiltz and Rossion, 2006; Yovel and Kanwisher, 2005], a process which has led to wide variability in localized ROI size. In other studies, when the localizer failed to reveal regions consistently the threshold has been manipulated to allow the localization of ROIs in the maximum number of subjects, with the result being widely variable thresholds in the literature (e.g., conservative- [Schiltz and Rossion, 2006]; liberal- [Ishai et al., 2005]), a practice that others suggest brings into question the objectivity and validity of the process [Genovese et al., 2002]. With this variation in statistical threshold comes a variability in ROI cluster size, with some groups reporting very large clusters of face-related activity [Ishai et al., 2005; Sorger et al., 2007]. Some have minimized these vast size differences by varying the statistical threshold and using a standard cluster size across subjects, verifying their results at several different cluster sizes [Jiang et al., 2006].

Our second goal was to determine if we could define a statistically optimal cluster size for face-related ROIs that is not dependent upon the empiric process of setting thresholds. Large ROIs may be particularly problematic because others have noted that face-selectivity decreases with increased cluster size [Golarai et al., 2007]. We used a statistical method that determined the cluster size with the highest face-selectivity, which we consider a “statistically optimal” ROI. The results show that an average cluster size of approximately 50 mm³ provides maximal face selectivity and, interestingly, this is true for all regions of the core system for face perception.

This cluster size of 50 mm³ is much smaller than the average size of face-related ROIs reported in the literature, with the normally reported range extending from 150 mm³ [Sorger et al., 2007] to 5000 mm³ [Ishai et al., 2004]. In addition, when looking at the maximal face-selectivity within individual ROIs, very few reach their maximal face-selectivity in clusters larger than 200 mm³ (Fig. 7B). This optimal cluster size of 50 mm³ cannot simply be the result of data smoothing, as functional scans were not spatially smoothed nor did they undergo any spatial transformations, all analyses being performed in native space. Interestingly, examination with high-field fMRI reveals smaller face- and object-related clusters within the FFA as defined at standard fMRI resolution [Grill-Spector et al., 2006]. Thus, the optimal cluster size we report (50 mm³), although smaller than currently reported values, may reflect the more face-selective clusters seen with high-field

fMRI. Two other groups have reported the use of a fixed cluster size for localizing face-related ROIs (9 voxels [Yi et al., 2006]; multiple fixed sizes [Jiang et al., 2006]) and we argue that such an approach will result in ROIs that are more face-selective than those localized with a threshold based on a fixed *t*-value (see Fig. 8). Using individually determined cluster sizes may provide even better face selectivity, but is more time-consuming.

We believe that these results show that localization and definition of face-selective areas can be accomplished both more sensitively and more selectively than with current methods. The *dynamic localizer* is more sensitive in the detection of face-responsive ROIs in both the core and extended systems, and provides more consistent localization of these regions across individual subjects. While this also increases the number of voxels activated according to traditional statistical threshold methods, it is possible to determine statistically optimal cluster sizes that are not vulnerable to manipulations in threshold, and also more face-selective than ROIs defined by traditional threshold criteria. Greater face-selectivity should enhance investigations of how neural responses in these ROIs vary with adaptation and other stimulus modifications, and better detection of these ROIs in individuals will enhance confidence in the results of fMRI investigations in single case-studies, such as those concerning prosopagnosia.

ACKNOWLEDGMENTS

C.J.F. is supported by a Canadian Institutes of Health Research Canada Graduate Scholarship Doctoral Research Award and a MSFHR Senior Graduate Studentship. G.I. is supported by MSFHR and the Alzheimer Society of Canada (ASC). J.J.S.B. is supported by a Canada Research Chair and a Senior Scholarship from the Michael Smith Foundation for Health Research. The authors would like to thank all the staff at the UBC MRI Research Centre.

REFERENCES

- Adolphs R, Tranel D, Damasio H, Damasio A (1994): Impaired recognition of emotion in facial expressions following bilateral damage to the human amygdala. *Nature* 372:669–672.
- Adolphs R, Damasio H, Tranel D, Damasio AR (1996): Cortical systems for the recognition of emotion in facial expressions. *J Neurosci* 16:7678–7687.
- Andrews TJ, Ewbank MP (2004): Distinct representations for facial identity and changeable aspects of faces in the human temporal lobe. *Neuroimage* 23:905–913.
- Avidan G, Hasson U, Malach R, Behrmann M (2005): Detailed exploration of face-related processing in congenital prosopagnosia, Part 2: Functional neuroimaging findings. *J Cogn Neurosci* 17:1150–1167.
- Barton JJ (2003): Disorders of face perception and recognition. *Neurol Clin* 21:521–548.
- Benton CP, Etchells PJ, Porter G, Clark AP, Penton-Voak IS, Nikolov SG (2007): Turning the other cheek: The viewpoint dependence of facial expression aftereffects. *Proc R Soc London B* 274:2131–2137.

- Brewer AA, Press WA, Logothetis NK, Wandell BA (2002): Visual areas in macaque cortex measured using functional magnetic resonance imaging. *J Neurosci* 22:10416–10426.
- Damasio A. (1985): Prosopagnosia. *Trends Neurosci* 8:132–135.
- de Renzi E (1986): Prosopagnosia in two patients with CT scan evidence of damage confined to the right hemisphere. *Neuropsychologia* 24:385–389.
- Eger E, Schyns PG, Kleinschmidt A (2004): Scale invariant adaptation in fusiform face-responsive regions. *Neuroimage* 22:232–242.
- Friston KJ, Rotshtein P, Geng JJ, Sterzer P, Henson RN (2006): A critique of functional localisers. *Neuroimage* 30:1077–1087.
- Gauthier I, Tarr MJ, Moylan J, Skudlarski P, Gore JC, Anderson AW (2000): The fusiform “face area” is part of a network that processes faces at the individual level. *J Cogn Neurosci* 12:495–504.
- Genovese CR, Lazar NA, Nichols T (2002): Thresholding of statistical maps in functional neuroimaging using the false discovery rate. *Neuroimage* 15:870–878.
- Gobbini MI, Haxby JV (2006): Neural response to the visual familiarity of faces. *Brain Res Bull* 71:76–82.
- Gobbini MI, Haxby JV (2007): Neural systems for recognition of familiar faces. *Neuropsychologia* 45:32–41.
- Golarai G, Ghahremani DG, Whitfield-Gabrieli S, Reiss A, Eberhardt JL, Gabrieli JD, Grill-Spector K (2007): Differential development of high-level visual cortex correlates with category-specific recognition memory. *Nat Neurosci* 10:512–522.
- Golby AJ, Gabrieli JD, Chiao JY, Eberhardt JL (2001): Differential responses in the fusiform region to same-race and other-race faces. *Nat Neurosci* 4:845–850.
- Grill-Spector K, Knouf N, Kanwisher N (2004): The fusiform face area subserves face perception, not generic within-category identification. *Nat Neurosci* 7:555–562.
- Grill-Spector K, Sayres R, Ress D (2006): High-resolution imaging reveals highly selective nonface clusters in the fusiform face area. *Nat Neurosci* 9:1177–1185.
- Haxby JV, Hoffman EA, Gobbini MI (2000): The distributed human neural system for face perception. *Trends Cogn Sci* 4:223–233.
- Ishai A, Ungerleider LG, Haxby JV (2000): Distributed neural systems for the generation of visual images. *Neuron* 28:979–990.
- Ishai A, Pessoa L, Bickle PC, Ungerleider LG (2004): Repetition suppression of faces is modulated by emotion. *Proc Natl Acad Sci USA* 101:9827–9832.
- Ishai A, Schmidt CF, Boesiger P (2005): Face perception is mediated by a distributed cortical network. *Brain Res Bull* 67:87–93.
- Jiang X, Rosen E, Zeffiro T, VanMeter J, Blanz V, Riesenhuber M (2006): Evaluation of a shape-based model of human face discrimination using fMRI and behavioral techniques. *Neuron* 50:159–172.
- Kanwisher N, McDermott J, Chun MM (1997): The fusiform face area: A module in human extrastriate cortex specialized for face perception. *J Neurosci* 17:4302–4311.
- Kilts CD, Egan G, Gideon DA, Ely TD, Hoffman JM (2003): Dissociable neural pathways are involved in the recognition of emotion in static and dynamic facial expressions. *Neuroimage* 18:156–168.
- Kosaka H, Omori M, Iidaka T, Murata T, Shimoyama T, Okada T, Sadato N, Yonekura Y, Wada Y (2003): Neural substrates participating in acquisition of facial familiarity: An fMRI study. *Neuroimage* 20:1734–1742.
- Landis T, Cummings J, Christen L, Boger J, Imhof H-G (1986): Are unilateral right posterior cerebral lesions sufficient to cause prosopagnosia? Clinical and radiological findings in six additional patients. *Cortex* 22:243–252.
- Mazard A, Schiltz C, Rossion B (2006): Recovery from adaptation to facial identity is larger for upright than inverted faces in the human occipito-temporal cortex. *Neuropsychologia* 44:912–922.
- McKeown MJ, Hanlon CA (2004): A post-processing/region of interest (ROI) method for discriminating patterns of activity in statistical maps of fMRI data. *J Neurosci Meth* 135:137–147.
- Meadows JC (1974): The anatomical basis of prosopagnosia. *J Neurol Neurosurg Psychiatry* 37:489–501.
- Ng B, Abugharbieh R, Palmer SJ, McKeown MJ (2007): Joint spatial denoising and active region of interest delineation in functional magnetic resonance imaging. *Conf Proc IEEE Eng Med Biol Soc2007:3404–3407*.
- Nieto-Castanon A, Ghosh SS, Tourville JA, Guenther FH (2003): Region of interest based analysis of functional imaging data. *Neuroimage* 19:1303–1316.
- Palermo R, Rhodes G (2007): Are you always on my mind? A review of how face perception and attention interact. *Neuropsychologia* 45:75–92.
- Pelphrey KA, Morris JP, Michelich CR, Allison T, McCarthy G (2005): Functional anatomy of biological motion perception in posterior temporal cortex: An fMRI study of eye, mouth and hand movements. *Cereb Cortex* 15:1866–1876.
- Perrett DI, Rolls ET, Caan W (1982): Visual neurones responsive to faces in the monkey temporal cortex. *Exp Brain Res* 47:329–342.
- Perrett DI, Oram MW, Harries MH, Bevan R, Hietanen JK, Benson PJ, Thomas S (1991): Viewer-centred and object-centred coding of heads in the macaque temporal cortex. *Exp Brain Res* 86:159–173.
- Puce A, Perrett D (2003): Electrophysiology and brain imaging of biological motion. *Philos Trans R Soc Lond B Biol Sci* 358:435–445.
- Puce A, Allison T, Bentin S, Gore JC, McCarthy G (1998): Temporal cortex activation in humans viewing eye and mouth movements. *J Neurosci* 18:2188–2199.
- Pyles JA, Garcia JO, Hoffman DD, Grossman ED (2007): Visual perception and neural correlates of novel ‘biological motion’. *Vision Res* 47:2786–2797.
- Reddy L, Kanwisher N (2007): Category selectivity in the ventral visual pathway confers robustness to clutter and diverted attention. *Curr Biol* 17:2067–2072.
- Rhodes G, Byatt G, Michie PT, Puce A (2004): Is the fusiform face area specialized for faces, individuation, or expert individuation? *J Cogn Neurosci* 16:189–203.
- Rickham PP (1964): Human experimentation. Code of Ethics of the World Medical Association. Declaration of Helsinki. *Br Med J* 2:177.
- Rossion B, Caldara R, Seghier M, Schuller A-M, Lazeyras F, Mayer E (2003): A network of occipito-temporal face-sensitive areas besides the right middle fusiform gyrus is necessary for normal face processing. *Brain* 126:2381–2395.
- Rotshtein P, Henson RN, Treves A, Driver J, Dolan RJ (2005): Morphing Marilyn into Maggie dissociates physical and identity face representations in the brain. *Nat Neurosci* 8:107–113.
- Sato W, Kochiyama T, Yoshikawa S, Naito E, Matsumura M (2004): Enhanced neural activity in response to dynamic facial expressions of emotion: An fMRI study. *Brain Res Cogn Brain Res* 20:81–91.
- Saxe R, Brett M, Kanwisher N (2006): Divide and conquer: A defense of functional localizers. *Neuroimage* 30:1088–1096, discussion 1097–1099.
- Schiltz C, Rossion B (2006): Faces are represented holistically in the human occipito-temporal cortex. *Neuroimage* 32:1385–1394.

- Schiltz C, Sorger B, Caldara R, Ahmed F, Mayer E, Goebel R, Rossion B (2006): Impaired face discrimination in acquired prosopagnosia is associated with abnormal response to individual faces in the right middle fusiform gyrus. *Cereb Cortex* 16:574–586.
- Schwarzlose RF, Baker CI, Kanwisher N (2005): Separate face and body selectivity on the fusiform gyrus. *J Neurosci* 25:11055–11059.
- Sorger B, Goebel R, Schiltz C, Rossion B (2007): Understanding the functional neuroanatomy of acquired prosopagnosia. *Neuroimage* 35:836–852.
- Spiridon M, Kanwisher N (2002): How distributed is visual category information in human occipito-temporal cortex? An fMRI study. *Neuron* 35:1157–1165.
- Thompson JC, Hardee JE, Panayiotou A, Crewther D, Puce A (2007): Common and distinct brain activation to viewing dynamic sequences of face and hand movements. *Neuroimage* 37:966–973.
- Wheaton KJ, Thompson JC, Syngeniotis A, Abbott DF, Puce A (2004): Viewing the motion of human body parts activates different regions of premotor, temporal, and parietal cortex. *Neuroimage* 22:277–288.
- Winston JS, Henson RN, Fine-Goulden MR, Dolan RJ (2004): fMRI-adaptation reveals dissociable neural representations of identity and expression in face perception. *J Neurophysiol* 92:1830–1839.
- Wohlschlagel AM, Specht K, Lie C, Mohlberg H, Wohlschlagel A, Bente K, Pietrzyk U, Stocker T, Zilles K, Amunts K, Fink GR. (2005): Linking retinotopic fMRI mapping and anatomical probability maps of human occipital areas V1 and V2. *Neuroimage* 26:73–82.
- Wojciulik E, Kanwisher N, Driver J (1998): Covert visual attention modulates face-specific activity in the human fusiform gyrus: fMRI study. *J Neurophysiol* 79:1574–1578.
- Yi DJ, Kelley TA, Marois R, Chun MM (2006): Attentional modulation of repetition attenuation is anatomically dissociable for scenes and faces. *Brain Res* 1080:53–62.
- Yovel G, Kanwisher N (2005): The neural basis of the behavioral face-inversion effect. *Curr Biol* 15:2256–2262.